Quantitative theory of the oxygen vacancy and carrier self-trapping in bulk TiO_2

Peter Deák,* Bálint Aradi, and Thomas Frauenheim
Bremen Center for Computational Materials Science, University of Bremen, PoB 330440, D-28334 Bremen, Germany
(Received 26 September 2012; published 15 November 2012)

Standard approximations of density functional theory often fail for defects in transition metal oxides. Despite its significance in applications and decades of research, the oxygen vacancy in TiO_2 is also poorly understood from the theory point of view. The Heyd-Scuseria-Ernzerhof functional (HSE06) provides a total energy that is a linear function of the occupation number (as it should be for the exact functional) also in TiO_2. This allows reproduction of the measured infrared absorption, photoluminescence, and thermal ionization data within ∼0.1 eV. From our calculations, a consistent and quantitative interpretation of the conflicting experiments emerges. Electron self-trapping in rutile makes the properties of the vacancy concentration dependent. In oxidized samples the vacancies are passivated by native Ti^{3+}/Ti^{4+} traps. This explains why electrons localized to the vacancy could only be observed after illumination at very low temperature in magnetic resonance experiments. In strongly reduced samples, electrons may stay localized in the vacancy and even the neutral state gives rise to two vertical electronic transitions (at 0.8 and 1.2 eV). The situation is much simpler in anatase, where only holes are self-trapped by O^{2-}/O^{1-} transitions. The oxygen vacancy is a shallower donor in anatase than in rutile.

DOI: 10.1103/PhysRevB.86.195206 PACS number(s): 71.55.Ht, 71.15.Mb, 71.35.Aa, 71.38.−k

I. INTRODUCTION

TiO_2 is very exciting both practically and as a model material for solid-state theory. Many new and emerging applications, from photocatalysis and photovoltaics to optoelectronics and spintronics, use it as a wide band-gap semiconductor. The actual width of the gap itself is an intriguing question. Low-temperature optical experiments yield 3.04 eV for rutile[1] and 3.42 eV for anatase,[2] while combined photo- and inverse photoelectron spectroscopy (PES) gives 3.3 eV for rutile.[3] The latter is relevant for the quasiparticle band gap of GW calculations, which is 3.34 eV for rutile and 3.56 for anatase.[4] Since solution of the Bethe-Salpeter equation (BSE) shows no significant lowering of the absorption threshold, the discrepancy between the optical and the photoelectron gap is probably due to strong electron-phonon coupling.[4–6] TiO_2 contains 0.5% (∼$3\cdot10^{20}$ cm^{-3}) oxygen vacancies (V_O), even if annealed at 1000 °C in oxygen.[7,8] Still, after decades of research, the properties of V_O remain elusive and controversial. Infrared absorption (IR) experiments on *strongly reduced rutile* indicated a double-donor behavior, with transitions at 0.75 and 1.18 eV.[9] Energies close to the latter value has been found in photoconductivity (PC) experiments[10] and by optical bleaching of thermoluminescence (TL).[11] Correlating with this (vertical) optical transition, thermal (adiabatic) transitions of 0.37 eV[11] and 0.48 eV[12] were reported by deep-level transient spectroscopy (DLTS) and thermally stimulated current (TSC) measurements, respectively. In recent electron paramagnetic resonance (EPR) studies on *oxidized rutile crystals under illumination*, a triplet signal has been assigned to the neutral and a doublet to the singly positive oxygen vacancy.[13,14] However, in contrast to the results quoted above, a thermal ionization energy of only ∼0.02 eV was reported.[14] We are not aware of IR data on *bulk anatase,* but a broad band, appearing after the quenching of the free-carrier absorption, at 3.0 eV was assigned to the oxygen vacancy.[15] It should be noted that annealing in oxygen diminishes the initial V_O concentration to the point when the remaining ones are compensated by residual impurities, and the color of the crystal changes from blue (due to free-carrier absorption) to yellowish and eventually colorless.[13–15] Therefore, it seems likely that the 3.0-eV transition is from the negatively charged impurity to the positively charged vacancy. In photoluminescence (PL), a band at 1.95 eV has correlated with the 3.0-eV absorption band, while another at 2.15 eV was attributed to the self-trapped exciton.[16] Hall measurements indicate a thermal activation energy of 0.004 eV for *n*-type carrier generation in anatase crystals of bluish hue.[17] Vacancy-related EPR signals in anatase were assigned to the positive charge state only.[18,19] PES is probing the surface layer and, in contrast to IR absorption, yields only a single broad peak in the gap. This is at 0.7–0.9 eV below the conduction band (CB) on the rutile (110) surface and is confirmed in electron-energy-loss spectroscopy.[20–24] It is agreed that the observed defect state on rutile (110) belongs to Ti atoms in the 3^+ oxidation state; however, it is being debated whether these are subsurface Ti interstitials[25] or the Ti neighbors of a surface oxygen vacancy[26] or both.[27] Resonant x-ray PES on anatase shows a broad asymmetric peak at ∼1.1 eV, both on (101) and (001) surfaces,[24] probably because oxygen vacancies in anatase prefer subsurface sites.[28]

TiO_2 is a good testing ground for electronic structure methods beyond the standard local (local density) and semilocal (generalized gradient) approximations (LDA and GGA, respectively) of density functional theory (DFT). The electron-self-interaction error in the latter gives rise to a tendency for delocalization, and results in a total energy that is a convex function of the fractional occupation number (instead of being linear like the exact functional).[29,30] On the one hand, this leads to the underestimation of the band gap and defect levels, which are observed in the gap, appear as resonances in the bands, leading to a qualitatively wrong description of the defect behavior.[31,32] The oxygen vacancy in TiO_2 is just such a case.[33] On the other hand, small polaronic states are suppressed in doped oxides in general[30,34,35] and are missed completely in TiO_2.[36] As an *ab initio* many-body

treatment is currently unaffordable for large TiO_2 supercells, much effort has been devoted to the study of V_O in TiO_2 by extending the standard approximations in a semiempirical manner. Most of these employ varying Hubbard U terms to increase localization.[37–44] The lattice constants are severely influenced, the gap cannot be restored (for reasonable U values) with these methods, and a consistent agreement among such theories and with experiment could not be achieved so far. The Hartree-Fock (HF) exchange gives a concave total energy and overestimates the gap and the localization.[29,30] Therefore, hybrid functionals with a mixture of GGA and HF exchange may represent a compromise and have also been applied to V_O in TiO_2.[37,45] Although all these hybrids increase the gap, their predictive ability is not necessarily better. Improvement over standard DFT can only be expected if they are free of the electron-self-interaction error, i.e., if their total energy is linear (as a function of the occupation numbers). It has been shown that besides exact exchange, screening is also important to obtain a functional with linear behavior.[29] This is taken into account by the screened HSE06 hybrid functional, which mixes 25% HF exchange to short-range interactions only.[46] The screening parameter, 0.2 $Å^{-1}$, has been determined to best reproduce *both* ground-state properties and the electronic structure in a large set of *semiconductors*. This semiempirical method may not be necessarily transferable to systems where the screening cannot be described in such a simple manner;[47] however, it was shown that in the case of bulk group-IV semiconductors, it provides the desired linear approximation.[48] As a consequence, in these materials the entire bulk electronic structure was well reproduced (not only the gap), and the calculated defect levels were within 0.1 eV of the experimental values. Calculations on rutile and anatase have also found linear behavior[36] and resulted in lattice constants better than LDA and the density of states was in very good agreement with GW and PES results.[49] They were also able to reproduce the experimentally observed, differing polaronic effects in Nb- and Al-doped rutile and anatase, which were missed by GGA + U and other hybrid (B3LYP) calculations. It should be noted that the hybrids used in Refs. 37 and 45 apply 20% HF-exchange and are still convex approximations,[50] whereas the so-called PBE0 hybrid functional (based on the Perdew-Burke-Enzerhof GGA functional), which has the same mixing as in HSE but over the full range, is concave in TiO_2.

In this paper we will confirm that the HSE06 functional is linear and also capable of a consistent and quantitative explanation of the experiments on V_O in TiO_2. Calculations have been performed before by a modified HSE-type functional,[33,51] by tuning the mixing ratio to fit the *optical* band gap of rutile. Such a fitting is not justified,[52] and the GW + BSE results[4,5] indicate that the optical gap of TiO_2 should *not* be reproduced by solving the electron problem alone. In addition, the downscaling of the mixing parameter to 20% causes deviation from the linearity.[36] Finally, we note that in a very recent paper, V_O has been investigated by the screened exact-exchange method.[53] While this is conceptually a good approach, for some reason spin-polarized calculations on the neutral vacancy were found to give results identical with the closed-shell solution. This is in strong contrast with the results presented here.

II. METHODS

Our calculations have been carried out with the Vienna *Ab initio* Simulation Package (VASP) 5.2.12, using the projector-augmented-wave method,[54] with the Ti3p states excluded from the core. A 420- (840-) eV cutoff was applied for the expansion of the wave functions (charge density). Results of the bulk calculations can be found in Refs. 36 and 49. The lattice constants obtained there are used in this work too: $a = 4.567$ Å; $c = 2.944$ Å for rutile and $a = 3.755$; $c = 9.561$ Å for anatase. Defect calculations in rutile were carried out in a $2 \times 2 \times 3$ (72-atom) multiple of the primitive cell with a 2^3 Monkhorst-Pack (MP) sampling[55] and in $2 \times 2 \times 5$ (120-atom), $2 \times 2 \times 7$ (168-atom), and $2\sqrt{2} \times 2\sqrt{2} \times 4$ (192-atom) supercells in the Γ approximation. In anatase the $2\sqrt{2} \times 2\sqrt{2} \times 1$ (96-atom) multiple of the Bravais cell was used with 2^3 MP sampling. Geometries were relaxed until the forces fell below 0.02 eV/Å. For charged defects both the total energy and the Kohn-Sham (KS) levels were corrected.[56] For the supercells with 72, 96, and 192 atoms and of more or less cubic shape, the methods of Lany and Zunger can be applied.[32,56] The dielectric constants were taken from the HSE06 calculations of Ref. 57. Energies have been aligned based on the average electrostatic potentials far from the defect, and band filling correction was applied for defect levels with dispersion.[32] Considering the excellent agreement of the HSE band structure with the GW results,[49] optical transitions between the five highest occupied and five lowest unoccupied states were calculated by solving the BSE, starting from the HSE06 ground-state solution.

III. CARRIER SELF-TRAPPING IN UNDOPED TiO_2

Our previous studies on n- and p-type dopants on a Ti site have shown[36] that rutile has a tendency to form small electron-polaron states, while small hole polaron states are formed in anatase but not vice versa. The rutile results have indicated electron self-trapping by a Ti^{4+}/Ti^{3+} acceptor transition in the vicinity of the donor impurity. The vertical ionization energy of the trapped electron to the CB edge was ∼1 eV. Holes in doped anatase were trapped by an O^{2-}/O^{1-} donor transition of a neighbor to the acceptor, with a vertical transition energy of ∼2 eV to the valence band (VB). So self-trapping can also be expected in undoped samples.

Our present calculations in the 192-atom rutile supercell results in a Ti^{4+}/Ti^{3+} electron trap (left panel in Fig. 1), with a vertical ionization energy of 0.5 eV (in the absence of an ionized donor impurity, the level is obviously shallower). Experiments confirm electron self-trapping in rutile,[58] and the vertical ionization energy of the self-trapped electron was estimated to be ∼0.3 eV in 4-nm rutile particles,[59] in reasonable agreement with our value. For the adiabatic ionization energy, we obtain a value <0.1 eV, which might explain why the trapped electron were released very fast when the temperature was raised.[58] In undoped anatase we do not find electron self-trapping but an O^{2-}/O^{1-} hole-trap (right panel of Fig. 1). The vertical and adiabatic ionization energies (with respect to the VB) are 1.3 and 0.2 eV, respectively, i.e., the hole trap of anatase is significantly deeper (and more localized) than the electron trap of rutile. Such traps have also been confirmed by experiment.[60] We have calculated the

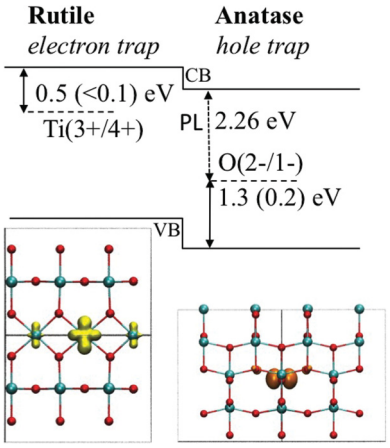

FIG. 1. (Color online) Native carrier traps in rutile (left) and anatase (right). The band gaps have been aligned according to Ref. 49. Dashed lines show the trap levels schematically. The calculated vertical (adiabatic) transition as well as the PL energy is indicated. The lower panel shows the spin distribution in the small electron-polaron state in rutile and the hole polaron state in anatase.

recombination energy of the self-trapped exciton in anatase to be 2.26 eV, in very good agreement with the observed 2.15-eV band in PL.[16] The differing tendency for carrier self-trapping will influence the state of the vacancy differently in the two modifications.

IV. THE VACANCY IN RUTILE

First, we have investigated the oxygen vacancy in a 72-atom rutile supercell. The closed-shell solution shown in Refs. 33 and 53, with two electrons localized in the space between the three Ti neighbors, is more than 0.3 eV higher in energy than the spin-polarized ground state, where the two equivalent Ti first neighbors trap an electron each in an antiferromagnetic spin-zero state [Fig. 2(a)], as also found in Ref. 42.

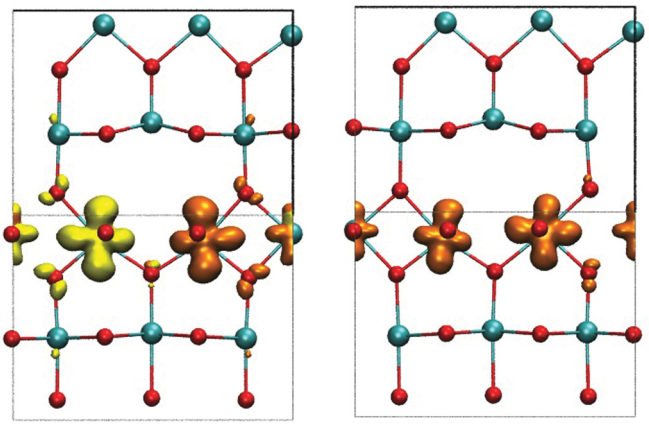

FIG. 2. (Color online) Spin-distribution in the antiferromagnetic singlet ground state of the oxygen vacancy in a $2 \times 2 \times 3$ rutile supercell (a) and in the triplet state 0.06 eV above it (b). Dark (orange/dark gray) and light (yellow/light gray) lobes correspond to the two spin channels. In the triplet state the distribution is identical for both unpaired electrons. Larger (cyan) and smaller (red) spheres represent Ti and O atoms, respectively.

A triplet state, in which both alpha electrons are shared between the equivalent neighbors [Fig. 2(b)], is higher by only 0.06 eV. The linearity of the total energy with the fractional occupation numbers can be checked by comparing the vertical ionization energy (energy difference of the neutral and ionized state, both calculated at the equilibrium geometry of the neutral one) with the KS energy of the electron state (occupied defect level in the neutral state) and with the KS energy of the hole state (unoccupied defect level in the ionized state). If the approximation is linear (and the electronic relaxation is small upon ionization), the three values should be equal.[30] With respect to the CB, the KS energies of the electron and hole states are at -0.80 and -0.82 eV in the antiferromagnetic singlet state, while the vertical ionization energy is -0.73. The small deviation of the latter is due to the inaccuracy of the charge correction in the total energy.[61] In all other cases given below, we find similar agreement, proving the near linearity and the lack of electron-self-interaction error in HSE06, if applied to TiO_2. The calculated level positions seem to agree with the values found in PES on the rutile (110) surface, indicating at least a contribution from bulk or subsurface vacancies. The adiabatic $(+/0)$ charge transition level of the singlet state is 0.08 eV below the CB, so at low temperature the neutral state can be stable. For the triplet state the KS energies of the electron states are 0.75 and 1.25 eV below the CB, very close to the IR absorption peaks (0.75 and 1.18 eV, respectively) attributed to V_O in reduced samples.

The nearly degenerate singlet and triplet states should both contribute to the IR spectrum, so we have calculated the imaginary part of the dielectric function in both cases by solving the BSE. Fig. 3 shows the range of defect transitions in comparison with the experimental IR spectrum.[9] The peak positions are well reproduced, however, in contrast to the original interpretation, the second main peak also arises from the neutral vacancy, V_O^0. The vertical ionization energy of the relaxed positive vacancy, V_O^+, is much deeper, so we assume that the second ionization contributes to the broadening and asymmetry of the main peak.[62] If bulk (or

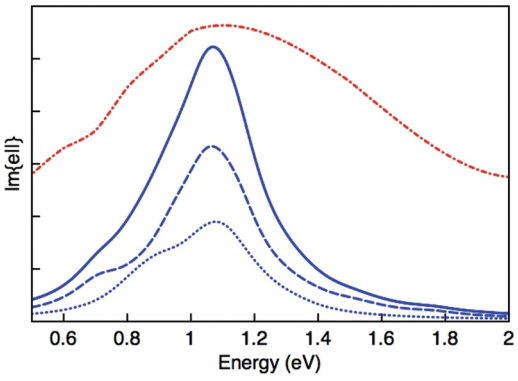

FIG. 3. (Color online) Imaginary part of the dielectric function, parallel with the main axis (and with the two equivalent Ti neighbors of the vacancy) in the 72-atom rutile cell with one neutral oxygen vacancy. Dotted and dashed (blue/medium gray) lines correspond to the singlet and triplet configurations, while the solid line is the sum of the curves. The dash-dotted (red/dark gray) line shows the normalized IR spectrum of Ref. 9, transformed to the present linear scale.

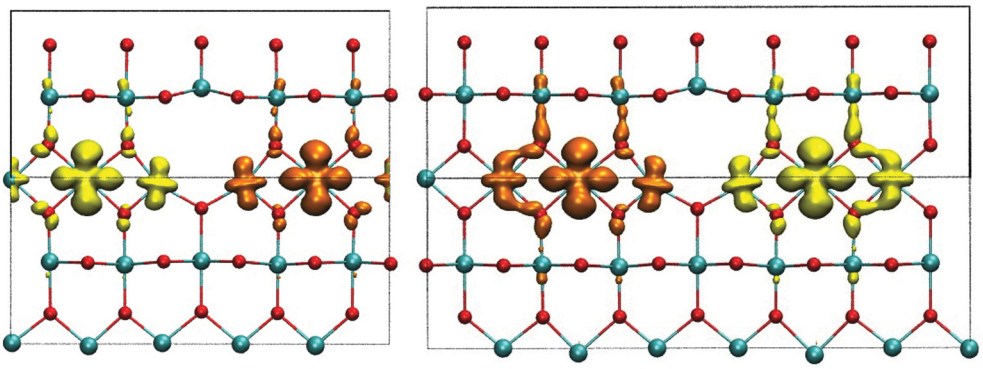

FIG. 4. (Color online) Spontaneous evolution of the singlet state (starting from the local geometry shown in Fig. 2(a)) in a $2 \times 2 \times 5$ (a) and a $2 \times 2 \times 7$ (b) supercell. In both cases, the result is a complex of V_O^{2+} and two self-trapped electrons. Dark (orange/dark gray) and light (yellow/light gray) lobes correspond to the two spin channels.

subsurface) vacancies show up in PES measurements, they should show a similar fine structure. The triplet state was observed in EPR under illumination, and the experiments confirm the state we find.[13,14] However, in those *oxidized samples*, the signal of both V_O^0 and V_O^+ disappeared upon a slight increase in temperature. Since the calculated adiabatic ionization energy of V_O^+ is 1.3 eV, this requires an explanation.

A single V_O in the 72-atom $2 \times 2 \times 3$ supercell corresponds to 2% oxygen deficiency, at least four times higher than in oxidized crystals. We observe a dispersion of about 0.15 eV in the vacancy level, indicating interaction between the repeated defects, and Fig. 2 shows significant contribution of a border atom to the vacancy state. Convergence tests in the $2 \times 2 \times 5$ and $2 \times 2 \times 7$ supercells show that with increasing size the electrons relocate to two equivalent second neighbors of the vacancy (Fig. 4), and the energy difference between the singlet and triplet states disappears (see Table I).

The result is essentially a complex of a dipositive vacancy, V_O^{2+}, and two nearby self-trapped electrons. We emphasize that this complex arises spontaneously: calculations in the larger cells have been started from the local geometry of the $2 \times 2 \times 3$ supercell.

Apparently, the "classic" vacancy state of Fig. 2 can only be found at a high concentration of the localized electrons. As Fig. 5(a) shows, even halving that by ionization in the $2 \times 2 \times 3$ supercell allows the remaining electron to leave the first neighbors. With careful choice of the starting geometry (as in Ref. 44), we could stabilize a triplet complex of V_O^+ and an electron trapped at a nearby Ti site [Fig. 5(b)]. Actually, that is even slightly more stable than the solutions shown in Fig. 2; nevertheless, the latter are definitely metastable and should occur in strongly reduced samples, as the ones used in Ref. 9. They are also to be expected in oxidized samples upon illumination at low temperature, for that will excite electrons from the VB (or from charged acceptor impurities) into the vacancy levels. However, in such samples both electrons dissociate from the vacancy at a slight increase in temperature, which allows the structural rearrangement, as witnessed in EPR.[14]

In the 192-atom $2\sqrt{2} \times 2\sqrt{2} \times 4$ supercell, a single V_O corresponds to 0.7% oxygen deficiency, closer to the value found in oxidized samples. As Fig. 6(a) shows, this size is sufficient to obtain the state in Fig. 4 spontaneously. Besides this complex and that in Fig. 5(b), however, we find now complexes where both self-trapped electrons are more remote from the V_O^{2+} and not even in the vacancy plane [Fig. 6(b)]. Such ($V_O^{2+} + 2e_{\text{trapped}}$) complexes are by ~0.2 eV lower in energy than the one shown in Fig. 2(a) but do not arise from it spontaneously at 0 K. The vertical transitions of the self-trapped electrons to the CB are ~1.1 eV, close to the value

TABLE I. Change of the total energy difference between the singlet and triplet state and of the splitting of the occupied KS states for the neutral vacancy in rutile supercells of increasing size. All values are in electron volts. The Γ-point approximation was used in this test.

	$2 \times 2 \times 3$ (Γ)	$2 \times 2 \times 5$ (Γ)	$2 \times 2 \times 7$ (Γ)
$\Delta E_{\text{singlet-triplet}}$	−0.040	−0.002	0.000
$\varepsilon^{\alpha}(\text{singlet}) - \varepsilon^{\beta}(\text{singlet})$	0.027	0.013	0.001
$\varepsilon^{\alpha 2}(\text{triplet}) - \varepsilon^{\alpha 1}(\text{triplet})$	0.479	0.274	0.026

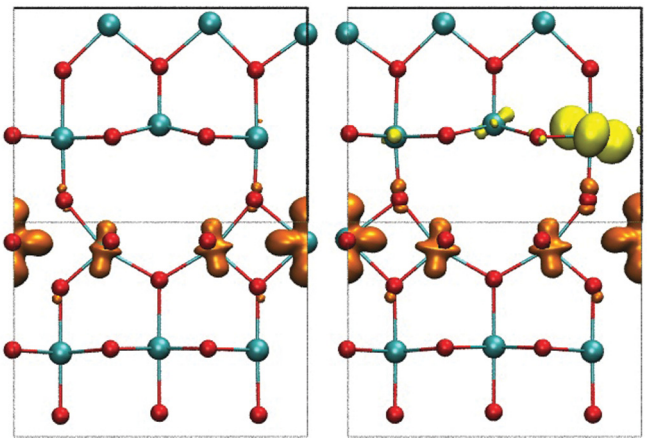

FIG. 5. (Color online) Spin distribution of the unpaired electron in the relaxed singly positive vacancy (a) and the two electrons (with same spin) in the complex of that with a nearby self-trapped electron (b).

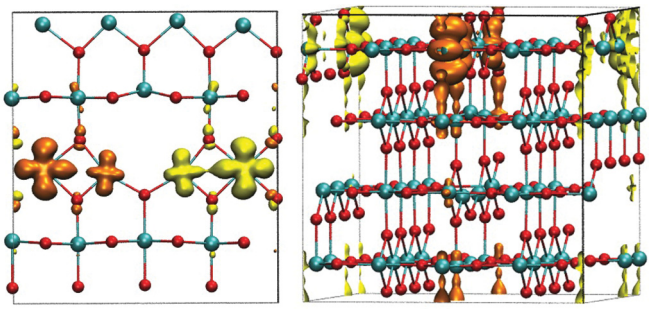

FIG. 6. (Color online) Complexes of V_O^{2+} and two self-trapped electrons in the $2\sqrt{2} \times 2\sqrt{2} \times 4$ supercell. Besides the complex in (a) and a similar one as in Fig. 5(b) (not shown here), both electrons can be farther away–as shown in (b)–from V_O^{2+}, which is at the center of the cells.

we have found near an ionized substitutional donor (Nb_{Ti}).[36] The adiabatic ionization energy is 0.4 eV. This is in very good agreement with the results of Refs. 11 and 12, so we believe that in Refs. 10 and 11 actually the vertical ionization of self-trapped electrons were detected (in slightly reduced samples).

V. THE VACANCY IN ANATASE

Without electron self-trapping, the oxygen vacancy in anatase is relatively simple. We obtain only solutions localized to the vacancy. In accord with the absence of a vacancy-related EPR signal, the neutral ground state is an "antiferromagnetic" singlet [Fig. 7(a)], and—unlike in Ref. 51—the third Ti neighbor also has some contribution. This state is strongly localized, so the size of the 96-atom supercell appears to be sufficient (the dispersion of the defect level was less than 0.02 eV).

We find a triplet state, 0.14 eV higher in total energy, in which the two localized electrons are shared by the neighbors in a bonding and in an antibonding state (Fig. 8). This is an excited state localized in the vacancy and not a weakly interacting pair of self-trapped electrons. Ionization leads to a configuration [Fig. 7(b)] in which the remaining electron is shared by the three neighbors on a bonding state (as in the excited triplet state). This state arises even before the nuclei are allowed to relax. The KS energy of the hole state is 0.53 eV, while the vertical ionization energy (calculated from the total energy difference) is 0.48 eV. The agreement demonstrates that HSE06 is a linear approximation also in anatase. We note that the calculated KS level of the electron state is at -0.85 eV (compared with -0.50 eV in Ref. 51). However, this should only be equal to the vertical ionization energy (in a linear approximation) if the relaxation of the electron system was negligible. This is clearly not the case here. So, the relevant value is the hole state energy, 0.5 eV. The second (vertical) ionization energy of V_O in anatase is 1.3 eV. These values are well in line with the broad, asymmetric PES peak at 1.1 eV. The defect band in the imaginary part of the dielectric constant (calculated with the BSE) has a similar band width (∼1.5 eV) as the (subsurface) vacancy band in the resonant PES of anatase.[24] We obtain the adiabatic $(0/+)$ transition level at 0.03 eV below the CB edge, again in line with the observed very shallow levels in noncompensated samples.[17]

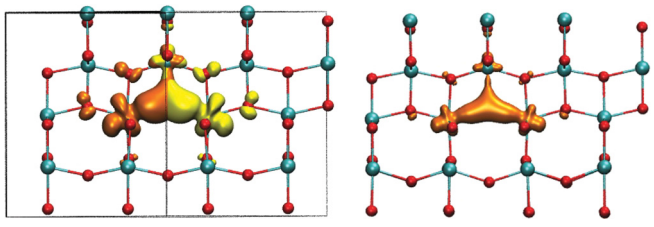

FIG. 7. (Color online) Spin distribution in the ground state of the neutral (a) and the positive (b) oxygen vacancy in anatase. Dark (orange/dark gray) and light (yellow/light yellow) lobes correspond to the two spin channels. Larger (cyan) and smaller (red) spheres represent Ti and O atoms, respectively.

TABLE II. The dependence of the formation energy (in electron volts) on the oxygen deficiency (in atomic percent for the neutral vacancy in TiO_2, under extreme O-rich and extreme Ti-rich conditions. The extreme limits correspond to O_2 molecule and Ti_2O_3 formation, respectively. The chemical potential of the O_2 molecule was taken at 0 K (values for 1000 °C and 1 atm of O_2 are in parentheses).

	O deficiency	O rich	Ti rich
Rutile	2.08%	5.45 (5.04)	1.65
Anatase	1.56%	5.33 (4.92)	1.54
Rutile	0.78%	5.19 (4.78)	1.42

VI. FORMATION ENERGY AND DONOR BEHAVIOR OF THE OXYGEN VACANCY IN INTRINSIC TiO_2

The calculated formation energy of the neutral V_O in TiO_2 is given at various concentrations in Table II. The O-rich data, relevant for annealing in O_2, extrapolate to 4.72 eV for 0.5% oxygen deficiency at 1000 °C, in good approximation to the experimental heat of formation, 4.55 eV (which also includes entropy).[7] In the extreme Ti-rich (O-poor) case, the formation energy in the dilute limit is less than 1.4 eV.

Finally, in Fig. 9, we summarize the calculated vertical (optical) and adiabatic (thermal) charge transition levels of both rutile and anatase. The adiabatic charge transition energies show that in rutile the neutral charge state of the vacancy is stable at low temperatures. However, the vacancy autoionizes if the temperature is sufficient for the structural rearrangement required to form the small polaron trapping state. The vacancy + self-trapped electron systems can only be ionized at the cost of 0.4 eV. Therefore, the isolated oxygen vacancy does not give rise to mobile carriers in the CB without illumination at room temperature. (It should be noted, though, that polaron-hopping may occur with an activation energy of ∼0.3 eV.[63]) In strongly reduced samples, the high concentration of localized electrons precludes the autoionization into native traps, and the $V(0/+)$ level is shallow enough for thermal ionization at room temperature, if dispersion is taken into account. In any case, exposure to visible light will give rise to free carriers. The second

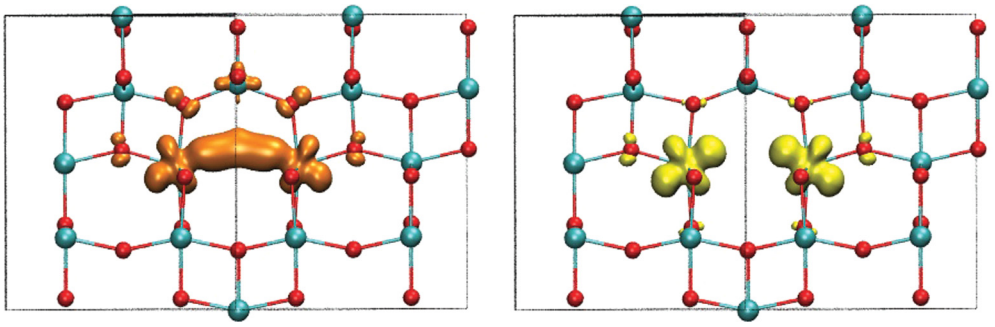

FIG. 8. (Color online) Spin distribution of the two occupied one-electron states in the excited triplet state of the neutral oxygen vacancy in anatase.

ionization level of the isolated V_O is rather deep in rutile, and its contribution to absorption and carrier generation is minor.

In anatase, both charge transition levels may be active (the thermal stability of the neutral state cannot be established even at 0 K, within the accuracy of the theory), and the vacancy should give rise to free carriers in the CB. It is interesting to note that—with the given alignment—the vertical charge transition levels of the isolated vacancies are nearly the same in rutile and anatase. The band offset, however, makes the oxygen vacancy a shallower donor in anatase. In strongly reduced samples, V_O provides for intrinsic n-type conductivity in both rutile and anatase, unless compensated by acceptorlike impurities. In oxidized samples the same is true for anatase but in rutile (due to autionization into native traps), conductivity in the dark cannot be activated at room temperature. The picture emerging from Fig. 9 is qualitatively, and to a great extent, also quantitatively in agreement with all observations.

VII. CONCLUSIONS

In summary, we have shown that the HSE06 functional (with the original parameters) provides the KS energies of the frontier orbitals in good agreement with the ionization energy of the oxygen vacancy in rutile and anatase, proving again that this semiempirical method is largely free of the electron self-interaction error also in TiO_2. This has allowed—besides a very good description of the properties of the perfect crystal[36,49]—a consistent interpretation of a wide range of experimental data. In particular, we have shown, that electrons are easily self-trapped in the perfect rutile lattice at a Ti site but can be thermally released with a low activation energy. The electrons of a vacancy also prefer such states. Next-neighbor Ti atoms to the vacancy can capture the electrons only if the vacancy concentration is high, or if the dipositive vacancy is populated with electrons at very low temperature. In this case an antiferromagnetic singlet and a triplet state coexist. The calculated imaginary part of the dielectric function is in good agreement with the IR spectrum observed in strongly reduced samples. In only slightly reduced samples, the electrons prefer to be trapped at sites further from the vacancy. The calculated vertical and adiabatic ionization energies of the self-trapped electrons near a vacancy are in good agreement with PC, TSC, DLTS, and TL measurements. In case of anatase, we find only hole self-traps, significantly deeper than the native electron traps. The calculated recombination energy of the self-trapped exciton is in excellent agreement with the value assigned in PL. The ground state of the vacancy is an antiferromagnetic singlet, with the two electrons shared by all three vacancy neighbors. The vertical ionization energies and the width of the defect band in the calculated imaginary dielectric function are in line with the results of resonant PES experiments, while the very shallow adiabatic charge transition level agrees with Hall effect measurements. We believe that the agreement of the calculated IR, PL, and thermal ionization data with the experimental values within 0.1 eV is unprecedented for a defect in metal oxides. We attribute this success of the HSE06 functional to the linearity of the total energy as a function of the fractional occupation numbers. Therefore, we recommend that the use of a hybrid functional should always be justified first by the linearity test.

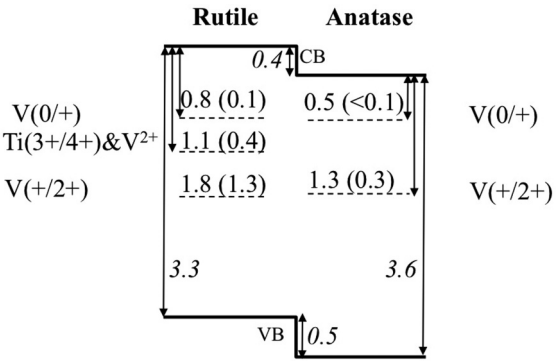

FIG. 9. Calculated vertical (adiabatic) charge transitions of the singlet vacancy in TiO_2 (in electron volts). The band gaps of rutile (left) and anatase (right) have been aligned according to Ref. 49. Note that the triplet state of the neutral vacancy in rutile is almost isoenergetic with the singlet state and has a second vertical transition at 1.3 eV.

ACKNOWLEDGMENTS

We are grateful for fruitful discussions with S. Lany, G. Kresse, A. Gali, and M. Arbab. The support of the Supercomputer Center of Northern Germany (HLRN Grant No. hbc00011) is acknowledged.

*Corresponding author: deak@bccms.uni-bremen.de

[1] J. Pascual, J. Camassel, and H. Mathieu, Phys. Rev. B **18**, 5606 (1978).

[2] H. Tang, F. Lévy, H. Berger, and P. E. Schmid, Phys. Rev. B **52**, 7771 (1995).

[3] Y. Tezuka, S. Shin, T. Ishii, T. Ejima, S. Suzuki, and S. Sato, J. Phys. Soc. Jpn. **63**, 347 (1994).

[4] W. Kang and M. S. Hybertsen, Phys. Rev. B **82**, 085203 (2010).

[5] L. Chiodo, J. M. García-Lastra, A. Iacomino, S. Ossicini, J. Zhao, H. Petek, and A. Rubio, Phys. Rev. B **82**, 045207 (2010).

[6] M. Landmann, E. Rauls, and W. G. Schmidt, J. Phys.: Condens. Matter **24**, 195503 (2012).

[7] P. Kofstad, *Non-Stoichiometry, Diffusion, and Electrical Conductivity in Binary Metal Oxides*, Chap. 8 (Wiley, New York, 1972).

[8] T. Bak, J. Nowotny, and M. K. Nowotny, J. Phys. Chem. B **11**, 21560 (2006).

[9] D. C. Cronemeyer, Phys. Rev. **113**, 1222 (1959).

[10] W.-T. Kim, C.-D. Kim, and Q. W. Choi, Phys. Rev. B **30**, 3625 (1984).

[11] A. K. Gosh, F. G. Wakim, and R. R. Addiss, Jr., Phys. Rev. **184**, 979 (1969).

[12] C. N. Druckworth, A. W. Brinkman, and J. Woods, Phys. Status Solidi A **75**, K99 (1983).

[13] S. Yang, L. E. Halliburton, A. Mannivanan, P. H. Bunton, D. B. Baker, M. Klemm, S. Horn, and A. Fujishima, Appl. Phys. Lett. **94**, 162114 (2009).

[14] F. D. Brandão, M. V. B. Pinheiro, G. M. Ribeiro, G. Medeiros-Ribeiro, and K. Krambock, Phys. Rev. B **80**, 235204 (2009).

[15] T. Sekiya, S. Kamei, and S. Kurita, J. Phys. Chem. Solids **61**, 1237 (2000).

[16] T. Sekiya, S. Kamei, and S. Kurita, J. Lumin. **87–89**, 1140 (2000).

[17] L. Forro, O. Chauvet, D. Emin, and L. Zuppiroli, J. Appl. Phys. **75**, 633 (1994).

[18] D. C. Hurum, A. G. Agrios, K. A. Gray, T. Rajh, and M. C. Thurnauer, J. Phys. Chem. B **107**, 4545 (2003).

[19] Z. Zhang, J. Long, X. Xie, H. Lin, Y. Zhou, R. Yuan, W. Dai, Z. Ding, X. Wang, and X. Fu, Chem. Phys. Chem. **13**, 1542 (2012).

[20] V. E. Heinrich, G. Dreselhaus, and H. J. Zieger, Phys. Rev. Lett. **36**, 1335 (1976).

[21] W. Göpel, J. A. Anderson, D. Frankel, M. Jaehning, K. Phillips, J. A. Schäfer, and G. Rocker, Surf. Sci. **139**, 333 (1984).

[22] R. G. Egdell, S. Eriksen and W. R. Flavell, Solid State Commun. **60**, 835 (1986).

[23] W. S. Epling, C. H. F. Peden, M.l A. Henderson, and U. Diebold, Surf. Sci. **412–413**, 333 (1998).

[24] A. G. Thomas, W. R. Flavell, A. K. Mallick, A. R. Kumarasinghe, D. Tsoutsou, N. Khan, C. Chatwin, S. Rayner, G. C. Smith, R. L. Stockbauer, S. Warren, T. K. Johal, S. Patel, D. Holland, A. Taleb, and F. Wiame, Phys. Rev. B **75**, 035105 (2007).

[25] S. Wendt, P. T. Sprunger, E. Lira, G. K. H. Madsen, Z. Li, J. Ø. Hansen, J. Matthiesen, A. Blekinge-Rasmussen, E. Lægsgaard, B. Hammer, and F. Besenbacher, Science **320**, 1755 (2008).

[26] C. M. Yim, C. L. Pang, and G. Thornton, Phys. Rev. Lett. **104**, 036806 (2010).

[27] K. Mitsuhara, H. Okumura, A. Visikovskiy, M. Takizawa, and Y. Kido, J. Chem. Phys. **136**, 124707 (2012).

[28] H. Cheng and A. Selloni, Phys. Rev. B **79**, 092101 (2009).

[29] X. Zheng, A. J. Cohen, P. Mori-Sánchez, X. Hu, and W. Yang, Phys. Rev. Lett. **107**, 026403 (2011).

[30] S. Lany and A. Zunger, Phys. Rev. B **80**, 085202 (2009).

[31] W. R. L. Lambrecht, Phys. Status Solidi B **248**, 1547 (2011).

[32] S. Lany and A. Zunger, Phys. Rev. B **78**, 235104 (2008).

[33] A. Janotti, J. B. Varley, P. Rinke, N. Umezawa, G. Kresse, and C. G. Van de Walle, Phys. Rev. B **81**, 085212 (2010).

[34] A. M. Stoneham, J. Gavartin, A. L. Shluger, A. V. Kimmel, D. Muñoz Ramo, H. M. Rønnow, G. Aeppli, and C. Renner, J. Phys.: Condens. Matter **19**, 255208 (2007).

[35] G. Pacchioni, F. Frigoli, D. Ricci, and J. A. Weil, Phys. Rev. B **63**, 054102 (2000).

[36] P. Deák, B. Aradi, and T. Frauenheim, Phys. Rev. B **83**, 155207 (2011).

[37] E. Finazzi, C. Di Valentin, G. Pacconi, and A. Selloni, J. Chem. Phys. **129**, 154113 (2008).

[38] G. Mattioli, F. Filippone, P. Alippi, and A. Amore Bonapasta, Phys. Rev. B **78**, 241201 (2008).

[39] G. Mattioli, P. Alippi, F. Filippone, R. Caminiti, and A. Amore Bonapasta, J. Phys. Chem. C **114**, 21694 (2010).

[40] B. J. Morgan and G. W. Watson, Phys. Rev. B **80**, 233102 (2009).

[41] B. J. Morgan and G. W. Watson, J. Phys. Chem. C **114**, 2321 (2010).

[42] K. Yang, Y. Dai, B. Huang, and Y. P. Feng, Phys. Rev. B **81**, 033202 (2010).

[43] S.-G. Park, B. Magyari-Köpe, and Y. Nishi, Phys. Rev. B **82**, 115109 (2010).

[44] J. Stausholm-Møller, H. H. Kristoffersen, B. Hinnemann, G. K. H. Madsen, and B. Hammer, J. Chem. Phys. **133**, 144708 (2010).

[45] M. M. Islam, T. Bredow, and A. Gerson, Phys. Rev. B **76**, 045217 (2007).

[46] J. Heyd, G. E. Scuseria, and M. Ernzerhof, J. Chem. Phys. **118**, 8207 (2003); J. A. V. Krukau, O. A. Vydrov, A. F. Izmaylov, and G. E. Scuseria, *ibid.* **125**, 224106 (2006).

[47] M. Jain, J. R. Chelikowsky, and S. G. Louie, Phys. Rev. Lett. **107**, 216806 (2011).

[48] P. Deák, B. Aradi, T. Frauenheim, E. Janzén, and A. Gali, Phys. Rev. B **81**, 153203 (2010).

[49] P. Deák, B. Aradi, and T. Frauenheim, J. Phys. Chem. C **115**, 3443 (2011).

[50] F. Bruneval, Phys. Rev. Lett. **103**, 176403 (2009).

[51] T. Yamamoto and T. Ohno, Phys. Chem. Chem. Phys. **14**, 589 (2012).

[52] R. Ramprasad, H. Zhu, P. Rinke, and M. Scheffler, Phys. Rev. Lett. **108**, 066404 (2012).

[53] H.-Y. Lee, S. J. Clark, and J. Robertson, Phys. Rev. B **86**, 075209 (2012).

[54] G. Kresse and J. Hafner, Phys. Rev. B **49**, 14251 (1994); G. Kresse and J. Furthmüller, *ibid.* **54**, 11169 (1996); G. Kresse and D. Joubert, *ibid.* **59**, 1758 (1999).

[55] H. J. Monkhorst and J. K. Pack, Phys. Rev. B **13**, 5188 (1976).

[56] S. Lany and A. Zunger, Phys. Rev. B **81**, 113201 (2010).

[57] B. Lee, C.-K. Lee, C. S. Hwang, and S. Han, Curr. Appl. Phys. **11**, S293 (2011).

[58] I. R. Macdonald, R. F. Howe, X. Zhang, and W. Zhou, J. Photochem. Photobiol., A **216**, 238 (2010).
[59] D. A. Panayotov, S. P. Burrows, and J. R. Morris, J. Phys. Chem. C **116**, 4535 (2012).
[60] T. Berger, M. Sterrer, O. Diwald, E. Knözinger, D. Panayotov, T. L. Thompson, and J. T. Yates, Jr., J. Phys. Chem. B **109**, 6061 (2005).
[61] H.-P. Komsa, T. T. Rantala, and A. Pasquarello, Phys. Rev. B **86**, 045112 (2012).
[62] No simple charge correction can be applied in calculating the dielectric function because some of the final states are also defect related.
[63] N. A. Deskins and M. Dupuis, Phys. Rev. B **75**, 195212 (2007).